Dalton Transactions

An international journal of inorganic chemistry

Accepted Manuscript

This article can be cited before page numbers have been issued, to do this please use: V. J. Eilrich, T. Grell, P. Lönnecke, C. Song, J. Matysik and E. Hey-Hawkins, *Dalton Trans.*, 2022, DOI: 10.1039/D2DT00202G.

ROYAL SOCIETY OF CHEMISTRY

rsc.li/dalton

View Article Online
DOI: 10.1039/D2DT00202G

ARTICLE

Gold(I) Complexes of Tetra-*tert*-butylcyclotetraphosphane

Volker Jens Eilrich,[a] Toni Grell,[b] Peter Lönnecke,[a] Chen Song,[c] Jörg Matysik[c] and Evamarie Hey-Hawkins *[a]

Received 00th January 20xx,
Accepted 00th January 20xx

DOI: 10.1039/x0xx00000x

The reaction of tetra-*tert*-butylcyclotetraphosphane *cyclo*-($P^tBu)_4$ (**L**) with one to four equivalents [AuCl(tht)] (tht = tetrahydrothiophene) leads to the gold(I) complexes [$(AuCl)_n$**L**] (*n* = 1–4, **1–4**) in which the ligand coordinates up to four gold(I) chloride fragments. Complexes **1–4** show dynamic behaviour with redistribution of {AuCl} moieties which was investigated by $^{31}P\{^1H\}$ NMR spectroscopy, DFT calculations and single crystal as well as powder X-ray diffraction.

Introduction

Cyclooligophosphanes *cyclo*-$(PR)_n$ (*n* = 3–6) have been intensively studies between 1960 and 1990, followed by a period of low activity.[1–3] However, these compounds have received renewed interest more recently, as they play an increasingly important role for example in P_4 activation and catalysis.[2–10] Although a large number of cyclooligophosphanes is known,[2–4,11] rational syntheses, reactivity studies and coordination chemistry are still limited, with the latter being mainly focused on metal carbonyls.[2] After developing rational syntheses for anionic phosphorus-rich compounds to study their coordination chemistry,[1,12–17] we have investigated the rational syntheses and the complexation behaviour of neutral oligophosphanes. Recent examples include the rational syntheses of *cyclo*-($P_4{}^tBu_3$)-containing compounds, namely {*cyclo*-($P_4{}^tBu_3$)}$_2$,[18] {*cyclo*-($P_4{}^tBu_3$)}$_2P^tBu$,[19] {*cyclo*-($P_4{}^tBu_3$)}$_2CH_2$ and E{*cyclo*-($P_4{}^tBu_3$)}$_3$ (E =As, Sb, Bi), starting from *cyclo*-($P_4{}^tBu_3$) synthons,[5,20] and the coordination chemistry of {*cyclo*-($P_4{}^tBu_3$)}$_2$[18] and its pentalene isomer. The oligodentate ligand {*cyclo*-($P_4{}^tBu_3$)}$_2$[18] can bind up to three gold(I) chloride fragments.[5,6] Furthermore, we have observed a distinct intramolecular dynamic behaviour of the corresponding gold(I) complexes as well as an exchange of gold(I) chloride fragments between different oligonuclear complexes, suggesting the presence of equilibria. Therefore, it was interesting to see whether smaller cyclooligophosphanes also display such a dynamic intermolecular behaviour.

Tetra-*tert*-butylcyclotetraphosphane *cyclo*-($P^tBu)_4$ was first described by Issleib and Hoffmann in 1966.[21] In contrast to the related cyclotriphosphane *cyclo*-($P^tBu)_3$,[22,23] which has been well studied,[2–4] only a few reactions have been reported for *cyclo*-($P^tBu)_4$, such as oxidations[24] and the conversion to cyclotriphosphanophosphonium cations.[25–27] The only known complexes of *cyclo*-($P^tBu)_4$ are two gold(I) bromido complexes which were described in 1996.[28] However, the authors employed gold(III) bromide which resulted in low yields, as gold(III) needs to be reduced to gold(I) first, presumably *via* oxidation of the cyclotetraphosphane. Comparable to the ring cleavage of *cyclo*-($P^tBu)_3$,[23,29] this leads to degradation of *cyclo*-($P^tBu)_4$, causing the relatively low yields compared to complexations of gold(I) by other phosphanes.[5,6] Furthermore, no full characterisation was reported. Although the authors were able to simulate a $^{31}P\{^1H\}$ NMR spectrum deducing 1,2-coordination (*trans*) in the dinuclear complex [$(AuBr)_2${*cyclo*-($P^tBu)_4$}], the spectrum itself indicates that there is another species present which was not described by the authors.

We have prepared a series of gold(I) complexes [$(AuCl)_n${*cyclo*-($P^tBu)_4$}] (*n* = 1–4) of the prototypic cyclooligophosphane *cyclo*-($P^tBu)_4$ with one to four gold(I) chloride fragments (compounds **1–4**) to understand the coordination chemistry as well as the dynamic behaviour of gold(I) cyclooligophosphane complexes in more detail.

Results and discussion

The reaction of cyclotetraphosphane **L** with one equivalent [AuCl(tht)] (tht = tetrahydrothiophene) gives the mononuclear gold complex [(AuCl)**L**] (**1**) (Scheme 1). **1** is a colourless to pale yellow compound which is fairly soluble in THF, benzene and toluene and poorly soluble in *n*-hexane. Complex **1** crystallised in two different polymorphs (crystal growth in THF/*n*-hexane 1:1 (v/v) or rapid precipitation gave metastable **1**–β that slowly converts to **1**–α which is also formed by slow crystallisation in THF) which contain one half (**1**–β, $P2_1/m$, Z' = 0.5, Fig. 1) or three (**1**–α, $P2_1/c$, Z' = 3) symmetry-independent molecules. In both polymorphs, the gold(I) chloride fragment is coordinated by one phosphorus atom, resulting in a monometallic monodentate

[a] Universität Leipzig, Fakultät für Chemie und Mineralogie, Institut für Anorganische Chemie, Johannisallee 29, 04103 Leipzig, Germany. Email: hey@uni-leipzig.de
[b] Dipartimento di Chimica, Università degli Studi di Milano, Via Camillo Golgi 19, 20131 Milano, Italy.
[c] Universität Leipzig, Fakultät für Chemie und Mineralogie, Institut für Analytische Chemie, Linnéstraße 3, 04103 Leipzig, Germany.

† Electronic Supplementary Information (ESI) available. For ESI and crystallographic data in CIF or other electronic formats see DOI: 10.1039/x0xx00000x

View Article Online DOI: 10.1039/D2DT00202G

complex with gold in a linear coordination environment. The Au–P bond lengths in both polymorphs (2.231(1) Å – 2.239(1) Å) are in the range of similar complexes.[5,6,30–32] The P–P bond lengths (2.192(2) Å – 2.226(2) Å) are also in the expected range.[33]

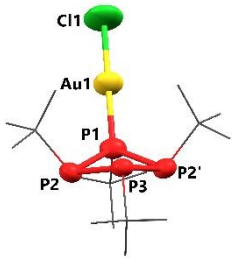

Fig. 1 Molecular structure of **1** (exemplarily shown for the β polymorph). Hydrogen atoms are omitted for clarity, *tert*-butyl groups are shown as wireframes. Thermal ellipsoids are shown at 50 % probability level. Selected bond lengths [Å] and angles [°]: Au1–P1 2.233(2), Au1–Cl1 2.263(3), P1–P2 2.192(2), P1–Au1–Cl1 179.2(1), P1–P2–P3 86.82(7).

In accordance with the molecular structure observed in the solid state, the $^{31}P\{^{1}H\}$ NMR spectrum of **1** (Fig. S17, ESI) is governed by an AM_2X spin system. The coupling constants and chemical shifts were determined by automated line-shape analysis (for full parameter set, s. Experimental Section). The resonances are shifted downfield compared to the free ligand **L**. In addition to the resonances of compound **1** (97.7 %), traces of **L** and [$(AuCl)_2$**L**] (**2**) (ca. 1.2 % each) are observed, indicating a redistribution equilibrium of {AuCl} units (s. Eq. 1), as was already observed for gold(I) complexes of {*cyclo*-($P_4{}^tBu_3$)}$_2$.[5] The purity of **1** in the solid state was confirmed by a Rietveld refinement of polymorph **1**–β (details in ESI, Fig. S8 and Fig. S9).

$$2\ [(AuCl)_n\{cyclo\text{-}(P^tBu)_4\}] \rightleftharpoons [(AuCl)_{n+1}\{cyclo\text{-}(P^tBu)_4\}] + [(AuCl)_{n-1}\{cyclo\text{-}(P^tBu)_4\}]$$

Eq. 1 Equilibrium of complexes **1**–**4** (n = 1–3).

The addition of one further equivalent [AuCl(tht)] to **1** results in the formation of the corresponding dinuclear complex **2** (Scheme 1). **2** is also accessible directly from **L** and two equivalents of the gold(I) complex. In comparison to **1**, complex **2** is slightly less soluble in common solvents. Two coordination modes are possible and indeed observed for the dinuclear complex **2** in the $^{31}P\{^{1}H\}$ NMR spectrum (Fig. S20–Fig. S25), namely 1,2- (**2a**, *trans*, AA'XX' spin system) and 1,3-coordination (**2b**, *cis*, A_2B_2 spin system). The occurrence of traces of the mononuclear (**1**) and trinuclear complex (**3**, s. below) indicates a similar redistribution equilibrium for **2** as suggested for compound **1** (Eq. 1). The resonances in **2** are shifted further downfield with respect to **1** which is in accordance with the coordination of a second gold(I) chloride fragment. Heckmann, Binder *et al.* only reported the 1,2-coordination mode for the gold(I) bromide analogue [$(AuBr)_2$**L**]. However, additional signals besides the expected and discussed AA'XX' spin system are present in the depicted $^{31}P\{^{1}H\}$ NMR spectrum around –7 ppm, suggesting the presence of the second isomer of the gold(I) bromido complex also here.[28]

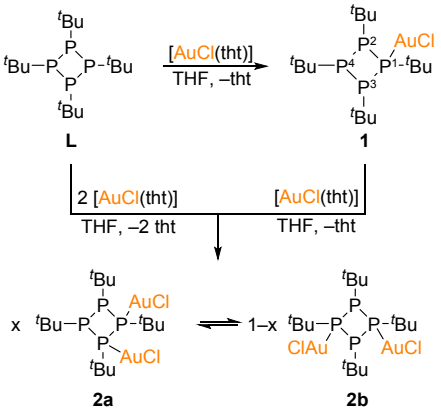

Scheme 1 Reaction of **L** with [AuCl(tht)] gives the mononuclear gold(I) complex **1**. Addition of one further equivalent furnishes the dinuclear complex **2** as two isomers with a 1,2- (**2a**) and a 1,3-coordination mode (**2b**).

All attempts to obtain NMR spectra of pure **2a** or **2b** in solution failed, suggesting an equilibrium between them. This is further supported by an observed solvent-dependency of the ratio **2a**:**2b** in the $^{31}P\{^{1}H\}$ NMR spectra. The ratio is related to the polarity of the solvent; it is found to be 1.26 in benzene-d^6 (ε_r = 2.28)[34] and shifts to 1.19 in toluene-d^8 (ε_r = 2.38)[34], 0.85 in THF-d^8 (ε_r = 7.52)[34] and 0.39 in acetonitrile-d^3 (ε_r = 36.64)[34] at 25 °C, favouring the more polar isomer **2b**. This is also supported by DFT calculations (DFT-D4//TPSSh/ZORA-def2-TZVP, s. ESI) which show a higher dipole moment for **2b** (12.7 D) than for **2a** (8.4 D) and furthermore a very low energy difference of ΔG(**2a**—**2b**) = –0.5 kJ/mol between the two complexes in benzene. Interestingly, the solvents used for NMR spectroscopy strongly influence the appearance of the A_2B_2 spin system. This type of spin system is only determined by the $^1J_{PP}$ coupling J_{AB} as well as the difference in chemical shift ($\Delta\nu_{AB}$) between ν_A and ν_B. $\Delta\nu_{AB}$ changes considerably when using acetonitrile-d^3 (5.73 ppm) or THF-d^8 (2.06 ppm) instead of benzene-d^6 (0.54 ppm) or toluene-d^8 (0.23 ppm) as solvent (Fig. S22–Fig. S25, ESI).

Even though the equilibrium between the isomers **2a** and **2b** will always lead to a mixture *in solution*, it was possible to obtain crystals of the isomer **2b** suitable for X-ray diffraction by recrystallisation from toluene. **2b** crystallises in the orthorhombic space group *Pnma* with two symmetry-independent half molecules in the asymmetric unit (Z' = 0.5 + 0.5; Fig. 2, top). Both molecules are in the 1,3-constitution and have similar parameters which are also comparable to complex **1**, involving a linear coordination of the gold(I) atom. Furthermore, an interesting disorder is observed in the crystal structure of **2b** (Fig. 2, bottom). One of the two symmetry-independent molecules (**A**) has a full occupancy of its two gold chloride groups (P1–Au1–Cl1, P3–Au2–Cl2; drawn in orange). In contrast to this, these Au–Cl fragments are only occupied to about 97 % in the second molecule (**B**, P4–Au3–Cl3 and P4'–Au3'–Cl3'; drawn in pink) and are additionally overlapped by

sites belonging to a further, differently oriented fragment (Au3F–Cl3F, occupied to 3 %; drawn in grey) which is connected to the remaining P atoms of the first molecule (**A**, P2–Au3F–Cl3F and P2'–Au3F'–Cl3F'). As both molecules are arranged alternatively in zig-zag chains along (010) (Fig. 2 and Fig. S7, ESI) this disorder leads to the statistical occurrence of the mononuclear and trinuclear complexes **1** and **3** (3.31 % each), and to a small fraction even of ligand **L** as well as tetranuclear complex **4** (0.06 % each, s. below) in addition to the *trans* isomer **2a** of the dinuclear complex **2b** (93.26 %). Besides this disorder, we detected a residual electron density maximum (Q1, 2.47) close to atom P5 (distance 2.49 Å), compatible with a linearly coordinated gold atom. Because its occupancy is rather low (< 1 %), it was not included in the final model of the structure. Nevertheless, this corresponds to a second disorder, which would, in combination with the first one mentioned above, effectively lead to a small fraction of molecules of the *trans* isomer (**2a**). This is remarkable as it means that the equilibrium observed between the different oligonuclear complexes (**L**, **1**–**4**) as well as between the two isomers **2a** and **2b** in solution is also partly reflected in this crystal structure. The discrepancy between the ratio of **2a** and **2b** in solution (1:1) and the solid state (< 1:1000) is most likely due to the packing. When crystals of **2b** are dissolved, the same mixture as in the NMR spectrum described above is observed which demonstrates the existence of the equilibria. It is entirely conceivable that also **2a** can be crystallised in pure form or as cocrystals with **2b** in a different structure if the right conditions were met. Co-crystallisation of different oligonuclear gold(I) oligophosphane complexes was also observed for gold(I) complexes of hexa-*tert*-butyl-bicyclo[3.3.0]octaphosphane $P_8{}^tBu_6$ (CSD code WUJREB) which underlines the dynamic behaviour of this type of compounds.[6]

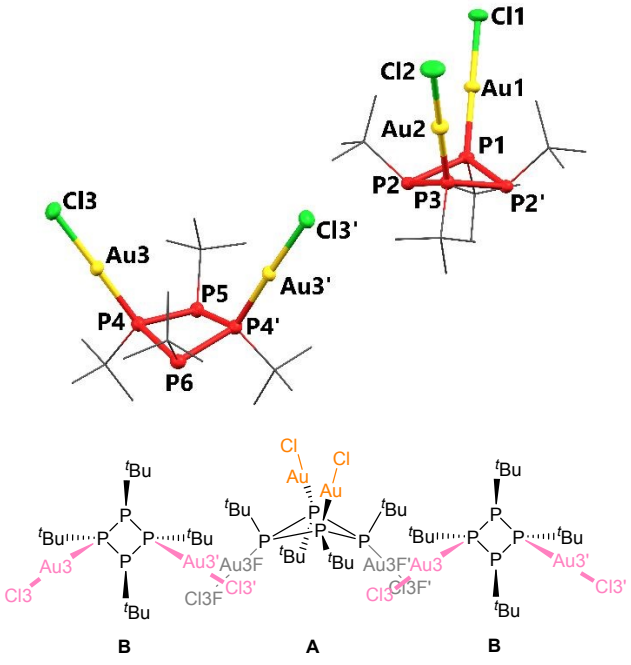

Fig. 2 Top: Molecular structure of **2b**. Hydrogen atoms are omitted and *tert*-butyl groups are drawn as wireframes for clarity. Thermal ellipsoids are shown at 50 % probability level. Bottom: Schematic excerpt of the discussed segment with the disorder in the crystal structure of **2b**. The {AuCl} fragments in the highlighted region occur with a ratio of ca. 97 % (pink) to 3 % (grey). Selected bond lengths [Å] and angles [°]: Au–P 2.230(1)–2.235(2), Au–Cl 2.266(1)–2.286(2), P–P 2.200(2)–2.216(2), P–Au–Cl 176.44(4)–179.09(5), P–P–P 86.27(5) –90.62(6).

When [AuCl(tht)] was used in a slight excess in the reaction with **L** (2.02 equiv.) to prepare **2**, single crystals (colourless needles) of the trinuclear complex **3** could be identified in the bulk of crystalline **2** (pale yellow prisms) obtained by recrystallisation in toluene. **3** crystallises together with 2.5 non-coordinating toluene molecules in the monoclinic space group *C*2/c with one symmetry-independent molecule per unit cell (Fig. 3). The Au–P (2.225(2) Å – 2.229(2) Å) and Au–Cl bond lengths (2.270(2) Å – 2.275(2) Å) are in the same range as in **1** and **2b**.

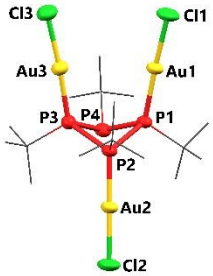

Fig. 3 Molecular structure of **3** · 2.5 C_7H_8. Hydrogen atoms and solvent molecules are omitted and *tert*-butyl groups are drawn as wireframes for clarity. Thermal ellipsoids are shown at 50 % probability level. Selected bond lengths [Å] and angles [°]: Au1–P1 2.225(2), Au1–Cl1 2.2270(2), P1–P2 2.224(3), P1–Au1–Cl1 177.42(9), P2–Au2–Cl2 178.79(9).

In contrast to the mono- (**1**) and dinuclear complex (**2**), the targeted preparation of **3** was unsuccessful. When three equivalents [AuCl(tht)] were added to **L**, a white, insoluble precipitate formed which was shown to be the tetranuclear complex **4** (s. below). The supernatant solution contained complex **2** (Scheme 2).

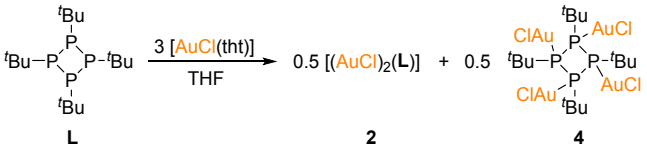

Scheme 2 Reaction of **L** with 3 equiv. [AuCl(tht)] gives the dinuclear gold(I) complex **2** in ca. 50 % yield, accompanied by the precipitation of white, insoluble powder of **4**.

However, it was possible to identify compound **3** and the $^{31}P\{^1H\}$ NMR spectrum of **2** (Fig. S21 and Fig. S22, ESI) and deduce its $^{31}P\{^1H\}$ NMR parameters by automated line-shape analysis after interfering oxides which were found in minute traces had been identified[‡] (s. ESI). It was found that the arithmetic means of the chemical shift of the resonances of compounds **L** and **1**–**3** in their $^{31}P\{^1H\}$ NMR spectra (in benzene-d^6) follow an empirical relation dependent on the number of gold(I) chloride fragments *n* (Eq. 2).

View Article Online DOI: 10.1039/D2DT00204C

$$\delta(^{31}\mathrm{P}) = (23.061\,n - 56.96)\ \mathrm{ppm}$$

Eq. 2 Empirical relation between the arithmetic mean of the chemical shifts $\delta(^{31}P)$ in benzene-d^6 and the number of gold(I) chloride fragments n for the compounds $[(AuCl)_n\{cyclo\text{-}(P^tBu)_4\}]$, n = 0–3 (**L**,**1**–**3**) (R^2 = 0.9992).

The expected chemical shift of compound **4** calculated by this equation (35.3 ppm) is in good agreement with the value determined experimentally by $^{31}P\{^1H\}$ (CP-MAS) NMR spectroscopy (arithmetic mean 29.4 ppm, s. Fig. S26, ESI).

Single crystals of compound **4** were obtained by layering a solution of the dinuclear complex **2** in *o*-difluorobenzene with a solution of [AuCl(tht)] in THF/toluene. Compound **4** crystallises in the monoclinic space group *C*2/*c* with one symmetry-independent molecule which is located on a crystallographic twofold axis (**4**, Fig. 4). The Au–P and P–P bond lengths as well as other structural parameters of the ligand are in the same range as those of **1**–**3**. Although the distances between the *cis*-oriented gold atoms *d*(Au1···Au1') (3.2959(5) Å) and *d*(Au2···Au2') (3.3183(4) Å) are relatively short, aurophilic interactions[35] can probably be excluded as the P–Au–Cl moieties lack the necessary perpendicular or antiparallel orientation.[36]

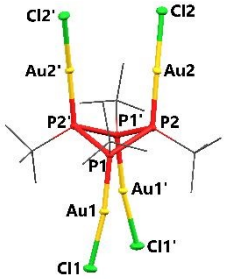

Fig. 4 Molecular structure of **4**. Hydrogen atoms are omitted and *tert*-butyl groups are drawn as wireframes for clarity. Thermal ellipsoids are shown at 50 % probability level. Selected bond lengths [Å] and angles [°]: Au1–P1, 2.2202(7); Au2–P2, 2.2220(7); Au1–Cl1 2.2795(7); Au2–Cl2, 2.2836(7), P1–Au1–Cl1 172.04(3), P2–Au2–Cl2 173.01(3), P1–P2–P1' 83.74(4).

Complex **4** is completely insoluble in all common solvents, including also unconventional solvents, such as α-methylnaphthalene or ionic liquids (1-butyl-1-methyl-pyrrolidinium-bis-(trifluormethylsulfonyl)-imid), limiting characterisation to the solid state. However, complex **4** is observed by ESI mass spectrometry when trifluoroacetic acid is added. The infrared spectrum shows the characteristic vibrations of the *tert*-butyl groups. But most importantly, Rietveld refinement of the PXRD pattern of the powder obtained when **L** is reacted with four equivalents [AuCl(tht)] confirmed that the substance is phase pure and in fact corresponds to the molecular structure of **4** described above (s. ESI).

Redistribution of {AuCl} Fragments

Gold(I) complexes are generally considered as labile and the occurrence of equilibria is a characteristic feature. These equilibria lead to dissociation of the complexes and redistribution of the ligands, as has been described for thiols and cyanides.[37–41] The novelty of the recent[5,6] and this work is that polydentate oligonuclear systems are involved, in which a redistribution of metal complex fragments occurs, leading to compounds with one more and one less gold chloride fragment (Eq. 1), thus shifting the view from a redistribution of the *ligands* to a redistribution of the *metal complex* fragments.

In order to get a deeper understanding of the nature of these equilibria, quantum chemical calculations (DFT-D4//TPSSh/ZORA-def2-TZVP, s. ESI) were conducted. The results showed that the reaction energy Δ*G* for each equilibrium is smaller than 0.05 kJ/mol. Therefore, the rearrangement of the {AuCl} fragments is energetically feasible.

Considering the redistribution equilibria also allows to understand the failure of the targeted preparation of **3**. Compound **3** is in equilibrium with compounds **2** and **4**, and due to its insolubility, **4** will be constantly removed from the equilibrium by precipitation, leading to full conversion of **3** to **2** and **4** (observed as insoluble white powder). A similar behaviour has been reported for the reaction of $[Au(CN)_2]^-$ with cysteine which is also driven by the extremely poor solubility of the product [Au(SCy)] (SCy = cysteinate).[40]

Furthermore, reaction of **L** with compound **2** results in redistribution with formation of **1** (Scheme 3). **1** is also formed in the reaction of **4** with an excess (3.64 equiv.) of **L**. If PPh_3 is used instead of **L** in the reaction with **2**, $[AuCl(PPh_3)]$[42] and **1** are identified as products, which confirms that ligand redistribution may also occur with other phosphanes. These findings are in line with the observation that $[Au(SR)]_n$ (SR = thiolate) oligomers react with further thiol to furnish monomeric complexes $[Au(SR)_2^-]$.[40,41]

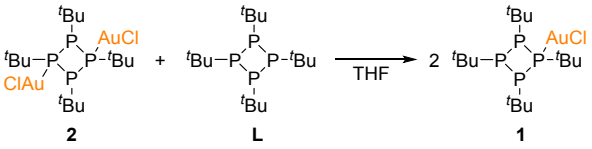

Scheme 3 The reaction of **L** with **2** (only one isomer is shown) leads to full conversion of **2** to **1**.

Conclusions

A series of oligonuclear gold complexes of cyclotetraphosphane *cyclo*-$(P^tBu)_4$ (**L**) was prepared, in which **L** coordinates one to four gold(I) chloride moieties. Complexes **1**–**4** have been characterised by X-ray diffraction techniques and NMR spectroscopy including automated line-shape analysis. The complexes show dynamic behaviour with redistribution of {AuCl} fragments, offering an interesting perspective in coordination chemistry as it changes the viewing from redistribution of ligands to redistribution of metal complex fragments. These findings were supported by theoretical calculations.

Experimental

All manipulations were performed using standard Schlenk techniques under nitrogen atmosphere unless stated

otherwise. Dry, oxygen-free solvents (THF, *n*-hexane, toluene) were obtained from an MBraun Solvent Purification System MB SPS-800. THF was further treated by dynamic drying employing molecular sieve (3 Å). Toluene and THF were stored over molecular sieve (4 Å) and *n*-hexane was stored over a potassium mirror. Solvents used for NMR spectroscopic measurements were distilled prior to use and stored over molecular sieve (4 Å or 3 Å (acetonitrile-d^3)). [AuCl(tht)][43] and *cyclo*-($P^tBu)_4$[21] were prepared following literature procedures. All reactions were performed with exclusion of light. NMR spectra were recorded on a Bruker Avance III HD 400 MHz spectrometer with a 5 mm TBO BB-1H/D/31P Z-GRD Z5610/004 probe head at 25 °C. The coupling constants *J* are reported in hertz (Hz) and are absolute values if no relative sign is indicated. The chemical shift (δ) is given in ppm. ^{1}H NMR spectra were either referenced to $SiMe_4$ as internal standard or to the solvent residual signal. Spectra of all other nuclei were referenced using the Ξ scale.[44] ^{31}P NMR spectra were recorded using 90° pulse angles and a D_1 time of 6.5 s. Automated line-shape analysis of NMR spectra was done using Daisy under Bruker's TopSpin[45], assuming a negative relative sign for $^1J_{PP}$. The ^{31}P cross-polarisation (CP) magic-angle-spinning (MAS) experiment was performed on a Bruker AVANCE-III 400 MHz WB NMR spectrometer equipped with a 4 mm double-resonance MAS probe and the ^{31}P chemical shift was referenced to external 85 % phosphoric acid. Mass spectrometry was performed on a Bruker Daltonics Esquire 3000 Plus, melting points were determined using a Gallenkamp MPD 350 BM 2.5 and are reported uncorrected. IR spectra were recorded on a Thermo Scientific Nicolet iS5 with a diamond ATR (400–4000 cm^{-1}), and for CHN analysis, a Heraeus Vario-EL oven was used.

Synthesis of [(AuCl){*cyclo*-($P^tBu)_4$}] (1)

A solution of 270 mg (0.842 mmol, 1.04 equiv.) [AuCl(tht)] in 50 ml THF and a solution of 285 mg (0.809 mmol) **L** in 10 ml THF were combined and stirred for 16 h at ambient temperature. The solvent was removed under reduced pressure and the obtained residue was recrystallised from *n*-hexane/THF (1:1, v/v). The pale-yellow precipitate was isolated and dried at 60 °C *in vacuo*, furnishing **1** (434 mg, 0.742 mmol, 92 %).

Mp. 193 °C (from *n*-hexane/THF, decomposition, sealed tube).

^{1}H NMR (400 MHz, benzene-d^6): δ 1.27 (d, $C_4H_9^{2,3}$, $^3J_{HP}$ = 14.8 Hz, 18H), 1.04 (d, $C_4H_9^1$, $^3J_{HP}$ = 18.9 Hz, 9H), 1.02 (d, $C_4H_9^4$, $^3J_{HP}$ = 13.7 Hz, 9H) ppm. (For numbering, see Scheme 1.)

^{13}C{^{1}H} NMR (101 MHz, benzene-d^6): δ 36.0 (m, $C(CH_3)_3^{1/4}$), 32.0 (m, $C(CH_3)_3^{2,3}$), 30.4 (m, $C(CH_3)_3^{1/4}$), 28.9 (m, $C(CH_3)_3^{2,3}$), 28.5 (m, $C(CH_3)_3^{1/4}$), 27.1 (m, $C(CH_3)_3^{1/4}$) ppm.

^{13}C{^{1}H,^{31}P} NMR (101 MHz, benzene-d^6, 28 °C): δ 35.7 ($C(CH_3)_3^{1/4}$), 31.6 ($C(CH_3)_3^{2,3}$), 30.0 ($C(CH_3)_3^{1/4}$), 28.5 ($C(CH_3)_3^{2,3}$), 28.2 ($C(CH_3)_3^{1/4}$), 26.7 ($C(CH_3)_3^{1/4}$) ppm.

^{31}P{^{1}H} NMR (162 MHz, benzene-d^6): AM_2X spin system (C_s, R = 0.56 %): δ_A = –9.32 (m, 1P, H_A = 3.25 Hz), δ_M = –34.71 (m, 2P, H_M = 3.61 Hz), δ_X = –55.54 (m, 1P, H_X = 3.39 Hz) ppm; J_{AM} = –200.63 Hz, J_{MX} = –153.90 Hz, J_{AX} = 5.50 Hz.

IR: $\tilde{\nu}$ 2944 (m), 2854 (m), 1456 (m), 1388 (w), 1360 (s), 1260 (w), 1168 (m), 1093 (w), 1009 (m), 934 (w), 865 (w), 802 (s), 598 (w), 578 (w), 548 (m) cm^{-1}.

HR-ESI(+)-MS (THF): *m*/*z* 585.1221 $[M+H]^+$.

CHN, found: C, 32.45; H, 6.42; N, 0.00. $C_{16}H_{36}AuClP_4$ requires C, 32.86; H, 6.21; N, 0.00 %.

TG-DTA: Thermolysis furnished elemental gold (Fig. S13, ESI).

Synthesis of [$(AuCl)_2${*cyclo*-($P^tBu)_4$}] (2)

64.8 mg (0.184 mmol) **L** and 113.3 mg (0.353 mmol, 1.92 equiv.) [AuCl(tht)] were suspended in 5 ml THF and stirred for 90 min at ambient temperature. The solvent of the clear yellow solution was removed under reduced pressure and the yellow residue (167.1 mg) was recrystallised in 7 ml toluene. Storing at 5 °C yielded single crystals. Isolation and drying at 60 °C *in vacuo* gave a mixture of **2a** and **2b** (83.3 mg, 0.102 mmol, 58 %).

Mp. decomposition above 156 °C (from toluene, sealed tube).

^{1}H NMR (400 MHz, benzene-d^6): δ 1.29 (m, 19H, C_4H_9 (**2b**)), 1.14 (m, 24H, C_4H_9 (**2a**)), 1.08 (m, 24H, C_4H_9 (**2a**)), 0.87 (m, 17H, C_4H_9 (**2b**)) ppm. **2a**:**2b** = 1.29.

^{13}C{^{1}H} NMR (101 MHz, benzene-d^6): δ 38.8 (m, $C(CH_3)_3$ (**2a**/**2b**)), 37.2 (m, $C(CH_3)_3$ (**2a**/**2b**)), 34.4 (m, $C(CH_3)_3$ (**2a**/**2b**)), 32.6 (m, $C(CH_3)_3$ (**2a**/**2b**)), 29.1 (m, $C(CH_3)_3$ (**2b**)), 28.8 (m, $C(CH_3)_3$ (**2a**)), 27.9 (m, $C(CH_3)_3$ (**2a**)), 27.4 (m, $C(CH_3)_3$ (**2b**)) ppm.

^{13}C{^{1}H,^{31}P} NMR (101 MHz, benzene-d^6, 28 °C): δ 38.4 ($C(CH_3)_3$ (**2a**/**2b**)), 36.7 ($C(CH_3)_3$ (**2a**/**2b**)), 33.9 ($C(CH_3)_3$ (**2a**/**2b**)), 32.1 ($C(CH_3)_3$ (**2a**/**2b**)), 28.6 ($C(CH_3)_3$ (**2b**)), 28.4 ($C(CH_3)_3$ (**2a**)), 27.4 ($C(CH_3)_3$ (**2a**)), 26.9 ($C(CH_3)_3$ (**2b**)) ppm.

^{31}P{^{1}H} NMR (162 MHz, benzene-d^6): **2a**: AA'XX' spin system (C_2, R = 0.84 %): $\delta_A = \delta_{A'}$ = 8.53 (m, 2P), $\delta_X = \delta_{X'}$ = –30.20 (m, 2P) ppm; $J_{AA'}$ = –168.59 Hz, J_{AX} = –220.31 Hz, $J_{XX'}$ = –119.95 Hz, $J_{AX'}$ = 0.48 Hz, H = 3.34 Hz; –8.6 (m, 3P; **2b**) ppm.

As the automated line-shape analysis of **2b** is more reliable with larger values of $\Delta\nu_{AB}$, the ^{31}P{^{1}H} NMR spectrum in acetonitrile-d^3 is presented here as well:

^{31}P{^{1}H} NMR (162 MHz, acetonitrile-d^3): **2b:** A_2B_2 spin system (C_{2v}, R = 1.03 %): δ_A = –5.16, δ_B = –10.89 ppm; J_{AB} = –206.30 Hz, H = 2.90 Hz; 7.9 (m, **2a**), –29.1 (m, **2a**) ppm.

IR: $\tilde{\nu}$ 2944 (m), 2855 (m), 1495 (w), 1454 (s), 1389 (m), 1360 (s), 1260 (w), 1160 (s), 1008 (m), 935 (w), 801 (m), 730 (m), 695 (w), 595 (w), 560 (m), 549 (m), 465 (w), 425 (w) cm^{-1}.

HR-ESI(+)-MS (THF): *m*/z 834.0476 $[M+NH_4]^+$.

CHN, found: C, 23.52; H, 4.15; N, 0.00. $C_{16}H_{36}Au_2Cl_2P_4$ requires C, 23.52; H, 4.44; N, 0.00 %.

[$(AuCl)_3${*cyclo*-($P^tBu)_4$}] (3)

Due to the reasons mentioned above, it was not possible to isolate pure complex **3**. However, the ^{31}P{^{1}H} NMR parameters were deduced from the ^{31}P{^{1}H} NMR spectrum of **2** (Fig. S21, ESI) as traces of **3** could be observed there.

^{31}P{^{1}H} NMR (162 MHz, benzene-d^6): AM_2X spin system (C_{2v})[§]: δ_A = 29.24 (1P), δ_M = 11.40 (2P), δ_X = –5.82 (1P) ppm; J_{AM} = –132.73 Hz, J_{AX} = 4.48 Hz, J_{MX} = –230.83 Hz; H = 2.85 Hz.

Synthesis of [$(AuCl)_4${*cyclo*-($P^tBu)_4$}] (4)

21.2 mg (0.026 mmol) **2** were dissolved in 7 ml *o*-difluorobenzene. This solution was layered with a solution of 52.8 mg (0.052 mmol, 2.02 equiv.) [AuCl(tht)] in 13 ml THF/toluene (8:5 (v/v)) and stored with exclusion of light. The resulting colourless single crystals were washed with 10 ml *n*-hexane and dried *in vacuo* (15.64 mg, 0.012 mmol, 47 %).
Mp. decomposition above 136 °C (sealed tube).
IR: $\tilde{\nu}$ 2953 (m), 2942 (m), 1456 (s), 1392 (m), 1364 (s), 1357 (s), 1207 (w), 1141 (s), 1015 (m), 933 (m), 793 (w), 579 (w), 530 (w), 519 (m), 437 (s) cm^{-1}.
HR-ESI(+)-MS (THF): *m*/z 1299.9578 $[M+NH_4]^+$.

Synthesis of 4 (powder)

10.446 mg (0.0296 mmol) **L** and 37.981 mg (0.1183 mmol, 4.00 equiv.) [AuCl(tht)] were stirred for 20 h in 5 ml THF at ambient conditions. After filtration, the precipitate was washed with 5 ml *n*-hexane and dried carefully *in vacuo*, yielding 19.6 mg white powder. The powder was examined by powder X-ray diffraction and showed to be a different polymorph or solvatomorph (Fig. S12, ESI). Further drying for two days at 10^{-3} mbar and 100 °C yielded a powder displaying the cell parameters of **4** (determined by powder X-ray diffraction (Fig. S11, ESI)).
$^{31}P\{^1H\}$ (CP-MAS, solid state): δ 30.3 (bs), 28.4 (bs) ppm.

Single Crystal X-Ray Diffraction

Single crystal X-ray diffraction data were collected with a GEMINI CCD diffractometer (RIGAKU). The radiation source was a molybdenum anode (Mo-K_α, $\lambda = 0.71073$ Å). The data reduction was carried out with CrysAlis Pro[46] using an empirical absorption correction with spherical harmonics (SCALE3 ABSPACK). The data for **1**–α, **1**–β, **2b**, **3** and **4** had been corrected with an analytical numeric absorption correction as well using a multifaceted crystal model based on expressions derived by Clark and Reid.[47] All structures were solved by dual space methods with SHELXT-2015 or SHELXT-2018.[48] Structure refinement was done with SHELXL-2018[49] by using full-matrix least-square routines against F^2 and anisotropic refinement of all non-hydrogen atoms. All hydrogen atoms were calculated on idealised positions. The pictures were generated with the programme Mercury.[50] In all pictures, hydrogen atoms were omitted for clarity and thermal ellipsoids are shown with 50% probability. The CCDC code for each single crystal structure in this article is listed in Table S1 (ESI). These data can be obtained free of charge *via* https://summary.ccdc.cam.ac.uk/structure-summary-form (or from the Cambridge Crystallographic Data Centre, 12 Union Road, Cambridge CB2 1EZ, UK; fax: (+44)1223-336-033; or deposit@ccdc.cam.uk).

Conflicts of interest

There are no conflicts to declare.

Acknowledgements

We thank Isa Kallweit for the crystallisation of **1**–α. Financial support from the Studienstiftung des deutschen Volkes (doctoral grant for VJE) is gratefully acknowledged.

Notes and references

‡ Baudler *et al.* report the $^1J_{PP}$ coupling constant J_{AM} in *cyclo*-$\{(P^tBu)_4O_3\}$ to be positive with a value of +151.4 Hz.[24] In fact, a negative relative sign was found to be correct.

§ No *R*-value is given as the $^{31}P\{^1H\}$ NMR spectrum which was used to determine the NMR parameters by automated line-shape analysis displayed **3** only as a side component.

1 S. Gómez-Ruiz and E. Hey-Hawkins, *Coord. Chem. Rev.*, 2011, **255**, 1360.
2 V. J. Eilrich and E. Hey-Hawkins, *Coord. Chem. Rev.*, 2021, **437**, 213749 and the references therein.
3 T. Wellnitz and C. Hering-Junghans, *Eur. J. Inorg. Chem.*, 2021, 8.
4 M. Baudler and K. Glinka, *Chem. Rev.*, 1993, **93**, 1623.
5 T. Grell and E. Hey-Hawkins, *Eur. J. Inorg. Chem.*, 2020, 732.
6 T. Grell and E. Hey-Hawkins, *Chem. – Eur. J.*, 2020, **26**, 1008.
7 T. Grell and E. Hey-Hawkins, *Inorg. Chem.*, 2020, **59**, 7487.
8 D. M. Yufanyi, T. Grell and E. Hey-Hawkins, *Eur. J. Inorg. Chem.*, 2019, 1557.
9 D. M. Yufanyi, T. Grell, M.-B. Sárosi, P. Lönnecke and E. Hey-Hawkins, *Pure Appl. Chem.*, 2019, **91**, 785.
10 A. Schumann, F. Reiß, H. Jiao, J. Rabeah, J.-E. Siewert, I. Krummenacher, H. Braunschweig and C. Hering-Junghans, *Chem. Sci.*, 2019, **10**, 7859.
11 M. Baudler, *Angew. Chem., Int. Ed. Engl.*, 1982, **21**, 492.
12 A. Schisler, P. Lönnecke, T. Gelbrich and E. Hey-Hawkins, *Dalton Trans.*, 2004, 2895.
13 A. Schisler, P. Lönnecke and E. Hey-Hawkins, *Inorg. Chem.*, 2005, **44**, 461.
14 S. Gómez-Ruiz, R. Wolf, S. Bauer, H. Bittig, A. Schisler, P. Lönnecke and E. Hey-Hawkins, *Chem. – Eur. J.*, 2008, **14**, 4511.
15 S. Gómez-Ruiz and E. Hey-Hawkins, *New J. Chem.*, 2010, **34**, 1525.
16 A. Kircali, R. Frank, S. Gómez-Ruiz, B. Kirchner and E. Hey-Hawkins, *ChemPlusChem*, 2012, **77**, 341.
17 A. Kırcalı Akdag, P. Lönnecke and E. Hey-Hawkins, *Z. Anorg. Allg. Chem.*, 2014, **640**, 271.
18 M. Baudler, J. Hellmann, P. Bachmann, K.-F. Tebbe, R. Fröhlich and M. Fehér, *Angew. Chem., Int. Ed. Engl.*, 1981, **20**, 406.
19 M. Baudler, M. Schnalke and C. Wiaterek, *Z. Anorg. Allg. Chem.*, 1990, **585**, 7.
20 V. J. Eilrich, T. Grell, P. Lönnecke and E. Hey-Hawkins, *Dalton Trans.*, 2021, **50**, 14144.
21 K. Issleib and M. Hoffmann, *Chem. Ber.*, 1966, **99**, 1320.
22 M. Baudler and C. Gruner, *Z. Naturforsch., B: Anorg. Chem., Org. Chem.*, 1976, **31**, 1311.
23 M. Baudler and J. Hellmann, *Z. Anorg. Allg. Chem.*, 1981, **480**, 129.
24 M. Baudler, A. Michels and M. Michels, *Z. Anorg. Allg. Chem.*, 2001, **627**, 31.
25 C. A. Dyker, N. Burford, G. Menard, M. D. Lumsden and A. Decken, *Inorg. Chem.*, 2007, **46**, 4277.
26 J. J. Weigand, N. Burford, R. J. Davidson, T. S. Cameron and P. Seelheim, *J. Am. Chem. Soc.*, 2009, **131**, 17943.
27 N. Burford, C. A. Dyker, M. Lumsden and A. Decken, *Angew. Chem., Int. Ed.*, 2005, **44**, 6196.
28 R. Schmidt, S. A. Moya, D. Villagra, H. Binder and Y. G. Heckmann, *Bol. Soc. Chil. Quim.*, 1996, **41**, 371.

View Article Online
DOI: 10.1039/D2DT00202G

29 M. Baudler and J. Hellmann, *Z. Anorg. Allg. Chem.*, 1984, **509**, 53.
30 D. M. Stefanescu, H. F. Yuen, D. S. Glück, J. A. Golen and A. L. Rheingold, *Angew. Chem., Int. Ed.*, 2003, **42**, 1046.
31 E. J. Fernández, M. C. Gimeno, P. G. Jones, A. Laguna, M. Laguna and J. M. López-de-Luzuriaga, *Angew. Chem., Int. Ed. Engl.*, 1994, **33**, 87.
32 H. Schmidbaur, T. Pollok, G. Reber and G. Müller, *Chem. Ber.*, 1988, **121**, 1345.
33 W. Weigand, A. W. Cordes and P. N. Swepston, *Acta Crystallogr., Sect. B: Struct. Crystallogr. Cryst. Chem.*, 1981, **37**, 1631.
34 C. Wohlfarth, in *CRC Handbook of Chemistry and Physics*. *A Ready-Reference Book of Chemical and Physical Data: 1995–1996*, ed. D. R. Lide, CRC Press, Boca Raton, 76th edn., 1995.
35 H. Schmidbaur, *Gold Bull.*, 2000, **33**, 3.
36 E. Andris, P. C. Andrikopoulos, J. Schulz, J. Turek, A. Růžička, J. Roithová and L. Rulíšek, *J. Am. Chem. Soc.*, 2018, **140**, 2316.
37 M. Naseem Akhtar, A. A. Isab, A. Al-Arfaj and M. Sakhawat Hussain, *Polyhedron*, 1997, **16**, 125.
38 P. N. Dickson, A. Wehrli and G. Geier, *Inorg. Chem.*, 1988, **27**, 2921.
39 A. L. Hormann, C. F. Shaw, III, D. W. Bennett and W. M. Reiff, *Inorg. Chem.*, 1986, **25**, 3953.
40 G. Lewis and C. F. Shaw, III, *Inorg. Chem.*, 1986, **25**, 58.
41 C. F. Shaw, III, J. Eldridge and M. P. Cancro, *J. Inorg. Biochem.*, 1981, **14**, 267.
42 T. E. Müller, J. C. Green, D. M. P. Mingos, C. M. McPartlin, C. Whittingham, D. J. Williams and T. M. Woodroffe, *J. Organomet. Chem.*, 1998, **551**, 313.
43 R. Uson, A. Laguna, M. Laguna, D. A. Briggs, H. H. Murray and J. P. Fackler, Jr., in *Inorganic Syntheses*, ed. H. D. Kaesz, John Wiley & Sons, Inc, Hoboken, 1989, vol. 26, pp. 85–91.
44 R. K. Harris, E. D. Becker, S. M. Cabral De Menezes, R. J. Goodfellow and P. Granger, *Concepts Magn. Reson.*, 2002, **14**, 326.
45 *DAISY, part of TopSpin 4.1.1*, Bruker BioSpin GmbH, Rheinstetten, 2020.
46 *Agilent, CrysAlis PRO*, Agilent Technologies Ltd., Yarnton, 2019.
47 R. C. Clark and J. S. Reid, *Acta Crystallogr., Sect. A: Found. Crystallogr.*, 1995, **51**, 887.
48 G. M. Sheldrick, *Acta Crystallogr., Sect. A: Found. Adv.*, 2015, **71**, 3.
49 G. M. Sheldrick, *Acta Crystallogr., Sect. C: Struct. Chem.*, 2015, **71**, 3.
50 C. F. Macrae, I. J. Bruno, J. A. Chisholm, P. R. Edgington, P. McCabe, E. Pidcock, L. Rodriguez-Monge, R. Taylor, J. van de Streek and P. A. Wood, *J. Appl. Crystallogr.*, 2008, **41**, 466.